Analysis of selected shear strength models based on research of beams without stirrups

Renata Kotynia[1], *Monika* Kaszubska[1,*]

[1] Faculty of Civil Engineering, Architecture and Environmental Engineering, Lodz University of Technology, Lodz, Poland

Abstract. The paper presents two theoretical models for calculating shear capacity of beams without stirrups. The analysis refers to slender concrete beams without transverse reinforcement flexurally reinforced with two types of bars: steel and composite (glass fiber reinforced polymer - GFRP). The research program included 29 single-span, simply supported T-section beams without transversal reinforcement. The three point loaded beams (with span to depth ratio a/d in the range of 2.9-3.0 referring to the slender beams). The four times lower modulus of elasticity of the GFRP reinforcement revealed a gentle, progressive shear - tension failure mode, opposite to the abrupt failure mode of the RC beams.

1 Introduction

The shear issue in beams or unidirectionally reinforced slabs is inseparably connected with bending and occurs in the support zones of these elements. The complex stress state due to the combination of shear force and bending moment is difficult to be clearly described. The mechanism of shear failure in the support zone of RC elements is conditioned by many factors. The first one is the sliding of both parts of the element crossed by the diagonal shear crack and rotation of a cut off part of the element, which is accompanied by the aggregate interlock action in the hardened cement. The second mechanism is caused by a dowel action of the longitudinal reinforcement. In the section where this reinforcement is crossed by the shear crack, it carries both longitudinal and perpendicular stresses. Moreover, the shear force is transferred by the uncracked concrete in the compressive zone and the direct strut action for point loads close to the support. Currently developed shear theories aim to take into account the complexity of the shear failure mechanism in the supporting zone of bent reinforced concrete elements without transverse reinforcement. Two different shear models [1] and [2] were used for a comparative analysis of experimental test results performed on the steel and GFRP reinforced beams without stirrups.

2 Experimental program

The research program consisted of 29 single-span, simply supported T-section beams, which in part was reported in [3], [4]. The T-section beams height was h_{tot} = 400 mm, width of the web: b_w = 150 mm and width and height of the flange: b_{eff} = 400 mm and h_f = 60 mm, respectively (Fig. 1).

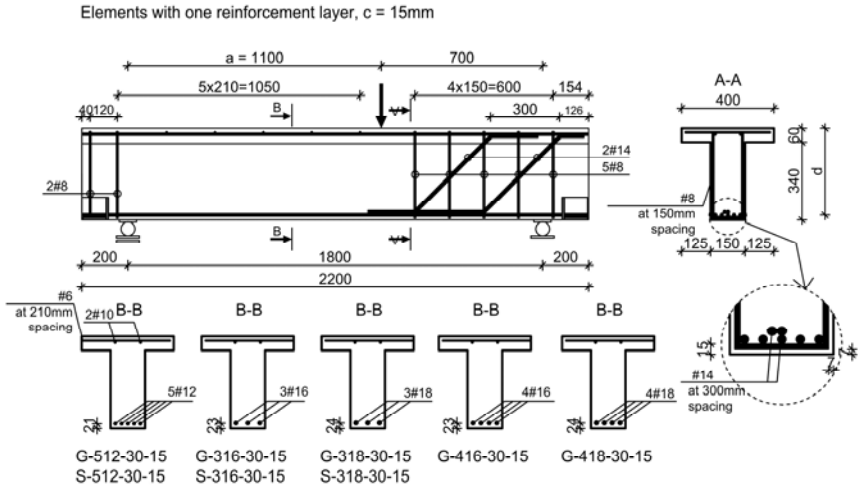

Fig. 1. Reinforcement of tested beams (series I, one reinforcement layer, c = 15 mm)

Beams of 2200 mm total length (and the axial span of 1800 mm) were tested under three point load applied 1100 mm from the support. Shear span to depth ratio a/d ranged between 2.9 and 3.0, which guaranteed slender concrete beams (Fig. 2).

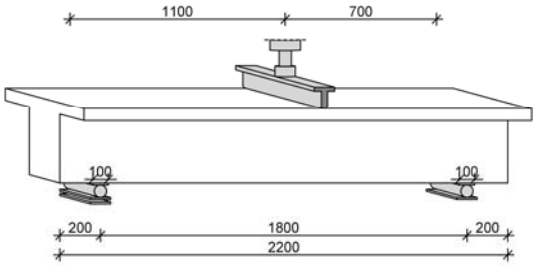

Fig. 2. Static scheme

The beams were divided into two experimental series. The average compressive strength of concrete in series I and II was f_{cm} = 31.8 MPa and f_{cm} = 35.9 MPa, respectively. The main aim of the research was a comparative analysis of members without shear reinforcement with GFRP and steel longitudinal reinforcement. One of the variable parameters was the longitudinal reinforcement ratio. Three values of ratio: $\rho_l \approx 1.0\%$, 1.4% and 1.8% were used in the tests (Table 1). For the lowest and medium reinforcement ratio, the influence of the number and diameter of bars were analyzed. Within each series, there were two values of concrete cover thickness (15 mm and 35 mm). Moreover, in the series I the lowest and highest reinforcement ratio were applied in one or two layers, which enabled the analysis of the number of reinforcement layers effect on the load capacity and ductility of the beams. The main reinforcement was made of straight bars with diameters of 12, 16 and 18 mm (Table 1). The top reinforcement consisted of two bars with a diameter of 10 mm connected by short transverse bars with a diameter of 6 mm, applied in a flange of T-section beam at a spacing of 210 mm. In each beam, the bottom and top reinforcement was made of the same material (respectively GFRP or steel). Along the whole length of the tested support zone, no transverse reinforcement was applied, whereas the opposite zone was protected against failure in shear by using the strong transverse reinforcement, made of steel stirrups of the nominal diameter of 8 mm, as well as bent steel bars with the diameter of 14 mm (Fig. 2).

Table 1. The details of tested specimens.

Elements	Series	d [mm]	a/d [-]	Number of bars [-]	Diameter of bars [mm]	A_l [mm^2]	ρ_l [%]	f_{ck} [MPa]
G-512-30-15	I	379	2.90	5	12	565	0.99	30.10
G-316-30-15		377	2.92	3	16	603	1.07	31.10
G-318-30-15		376	2.93	3	18	763	1.35	31.10
G-416-30-15		377	2.92	4	16	804	1.42	30.50
G-418-30-15		376	2.93	4	18	1018	1.80	31.10
S-512-30-15		379	2.90	5	12	565	0.99	31.10
S-316-30-15		377	2.92	3	16	603	1.07	32.30
S-318-30-15		376	2.93	3	18	763	1.35	33.80
G-312/212-30-15		367.8	2.99	5	12	565	1.02	32.30
G-318/118-30-15		367	3.00	4	18	1018	1.85	32.30
S-312/212-30-15		367.8	2.99	5	12	565	1.02	32.30
S-318/118-30-15		367	3.00	4	18	1018	1.85	33.80
G-512-30-35		359	3.06	5	12	565	1.05	31.10
G-316-30-35		357	3.08	3	16	603	1.13	30.50
G-318-30-35		356	3.09	3	18	763	1.43	30.50
G-418-30-35		356	3.09	4	18	1018	1.91	30.10
S-512-30-35		359	3.06	5	12	565	1.05	31.10
S-418-30-35		356	3.09	4	18	1018	1.91	33.80
G-316-35-15	II	377	2.92	3	16	603	1.07	37.05
G-318-35-15		376	2.93	3	18	763	1.35	37.05
G-416-35-15		377	2.92	4	16	804	1.42	36.02
S-512-35-15		379	2.90	5	12	565	0.99	34.95
S-316-35-15		377	2.92	3	16	603	1.07	36.33
S-318-35-15		376	2.93	3	18	763	1.35	37.35
G-316-35-35		357	3.08	3	16	603	1.13	35.00
G-418-35-35		356	3.09	4	18	1018	1.91	35.00
S-512-35-35		359	3.06	5	12	565	1.05	35.00
S-316-35-35		357	3.08	3	16	603	1.13	36.33
S-318-35-35		356	3.09	3	18	763	1.43	36.33

The beams were casted using ready mix concrete delivered from the local batch plant. The maximum aggregate size of concrete mixture was 8 mm diameter. The average modulus of elasticity and the maximum tensile strength registered in the test of GFRP bars was equal of 50.5 GPa (COV = 1.6%) and 1071 MPa (COV = 11.6%), respectively. The average value of the modulus of elasticity of steel bars was 201 GPa (COV = 3.7%), the average stress corresponding to the yield strength of 545 MPa (COV = 4.8%) and the average tensile strength 644 MPa (COV = 2.9%). For identification of members, a uniform nomenclature was applied: X-*nØ*/*mØ*-Y-Z, where: X is a type of reinforcement (GFRP, S-steel); *nØ* is a number of bars with diameter *Ø* in lower or *mØ* in the higher reinforcement level (for reinforcement applied in two layers); Y is the expected compressive concrete strength on cubic specimens in the series I and average on cylindrical ones in the series II; Z is the concrete cover thickness in mm (Table 1).

The four times lower modulus of elasticity of the GFRP reinforcement revealed a gentle, progressive shear - tensile failure mode, opposite to the abrupt failure mode of the RC beams. The detailed results and analysis of experimental research are available in [6].

3 Models

The undoubted advantage of the model [1] is its universality and possibility to be applied to elements without transversal reinforcement with steel and FRP longitudinal reinforcement. The basic assumption of the model is the initiation of shear, which begins with a diagonal cracking of the beam. After cracking, the crack width increases and the diagonal crack develops towards the upper edge of the beam. Failure occurs when the slope of this crack reaches the limit angle β_{CDC} at which both edges of the diagonal crack slip (Fig. 3).

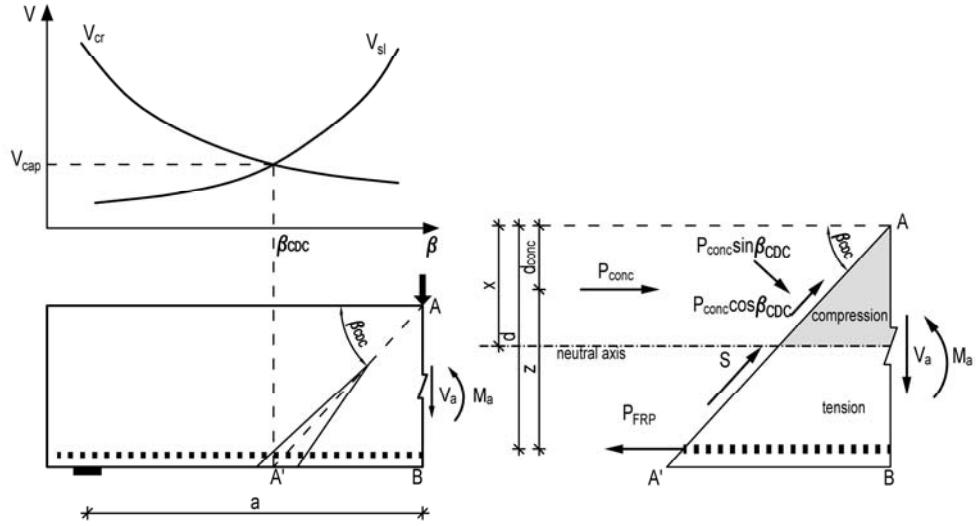

Fig. 3. The typical shear crack and forces acting on the fragment of beam in model [1]

The effect of the crack edge slip is the presence of force S, parallel to this plane. Based on the equilibrium of forces on the longitudinal axis of the beam and the moments relative to point A, compressive force in concrete is known. The capacity provided by the slip of the compression zone can be determined on the basis of shear stress, which is dependent on the compressive force in concrete and presliding shear friction failure properties A and B depending on the type of concrete. Part of the friction force is transferred by the action of the compressive force component in concrete parallel to the slip plane, and the remainder by the force S. Based on the above assumption, the equilibrium of forces and after certain transformations, the shear capacity is obtained according to formula (1).

$$V_{sl} = \frac{bxA}{1-[(B\sin\beta_{CDC} - \cos\beta_{CDC})\sin\beta_{CDC}]\cdot[\frac{M_a / V_a - d/\tan\beta_{CDC}}{z}]} \quad (1)$$

β_{CDC} angle is determined based on the internal forces V_a and M_a acting in the cross-section [7]:

$$\beta_{CDC} = -15\frac{M_a}{V_a d} + 89,7 \quad \text{if} \quad \frac{M_a}{V_a d} \le 3,14 \quad (2)$$

$$\beta_{CDC} = 42,6 \quad \text{if} \quad \frac{M_a}{V_a d} > 3,14 \quad (3)$$

The neutral axis depth is determined as:

$$x = \frac{E}{E_c}\rho_l d\left(\sqrt{1+\frac{2}{\frac{E}{E_c}\rho_l}}-1\right) \tag{4}$$

The modulus of elasticity of concrete is adopted according to ACI 1992 [3]:

$$E_c = 3320 f_c^{0,5} + 6900 \tag{5}$$

A linear distribution of normal stresses in the compression zone is assumed, so the arm of internal forces is calculated as:

$$z = d - \frac{x}{3} \tag{6}$$

Parameters A and B are adopted according to [8]:

$$A = 0,347 f_c^{0,665} \tag{7}$$

$$B = \frac{0,400 f_c - 0,37 - A}{0,25 f_c} \tag{8}$$

The model [2] based on the analysis of the diagonal crack development. The main crack proceeded by the cracking moment immediately reaches a constant height z_{cr} (9), which can be determined on the basis of the equilibrium of internal forces assuming that only the concrete transfers compressive stresses. The main crack, after reaching a height z_{cr}, stabilizes over the entire height z_{cr} and a further increase in load causes only an increase in its width and crack development in the horizontal direction (Fig. 4).

$$z_{cr} = (1+\rho_l\frac{E}{E_c} - \sqrt{2\rho_l\frac{E}{E_c}+(\rho_l\frac{E}{E_c})^2})d \tag{9}$$

A vertical displacement of the crack edge caused by its opening does not activate an aggregate interlock mechanism to transfer shear forces. An additional vertical displacement stimulates the development of a secondary horizontal branch of the crack and with the load increase leads to crack development at the reinforcement level.

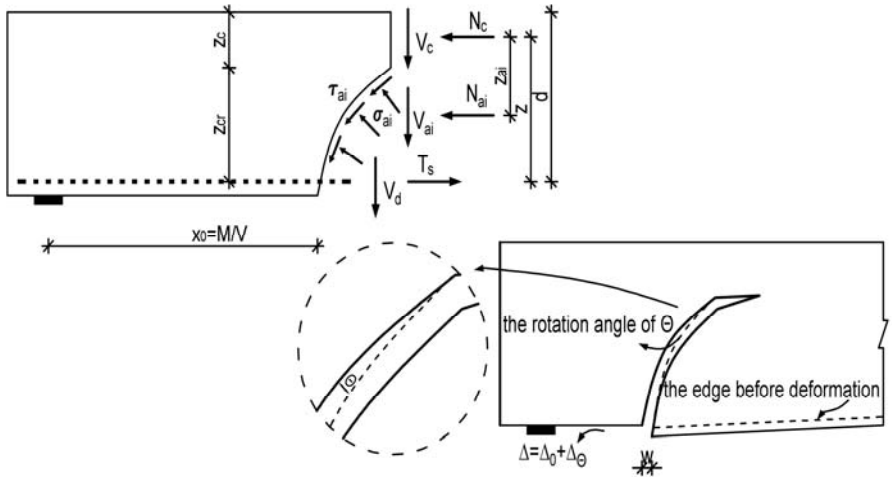

Fig. 4. The forces acting on the fragment of the beam and kinematic condition for critical crack

At some point, this process becomes sudden and uncontrolled, which leads to the increase of the crack width and loss of the shear capacity provided by the aggregate interlock. In this model, unstable crack development at a level of the main reinforcement constitutes the criterion of failure. After exceeding the critical value of the vertical displacement of the

diagonal crack Δ_{cr}, a horizontal crack along the longitudinal reinforcement appears (Fig. 4 – vertical displacement Δ). Based on the experimental results of concrete members without transversal reinforcement [2], the empirical formula Δ_{cr} was established:

$$\Delta_{cr} = \frac{25d}{30610\phi} + 0,0022 \le 0,025 \quad \text{mm} \tag{10}$$

Based on research [9], the distance between the main crack was determined as:

$$l_{cr} = \frac{z_{cr}}{1.28} \tag{11}$$

The aggregate interlock mechanism V_{ai} in the transverse force transfer was determined on the basis of Walraven's model [10].

$$V_{ai} = f_c^{0,56} z_{cr} b_w \frac{0,03}{w - 0,01}(-978\Delta_{cr}^{\ 2} + 85\Delta_{cr} - 0,27) \tag{12}$$

The crack width was determined on the level of longitudinal reinforcement as:

$$w = \frac{M}{(\frac{2}{3}d + \frac{1}{3}z_{cr})A_l E_s} l_{cr} \tag{13}$$

The dowel action force was determined according to the model [11]:

$$V_d = 1,64(b_w - n\phi)\phi^3\sqrt{f_c} \tag{14}$$

The contribution of uncracked concrete zone in shear capacity was determined in accordance with the assumptions of Mörsch's theory [12]. It was assumed that the position of the neutral axis does not change between two cracks, and the differences in compressive force are caused by tangential stresses along the neutral axis. The parabolic distribution of shear stress with the maximum value at the level of the neutral axis was assumed, hence the transverse force transferred through the compressive concrete zone is determined as:

$$V_c = \frac{2}{3}\frac{z_c}{z}V \tag{15}$$

According to model [2], the shear capacity is the sum of shear forces transferred by the uncracked compressive chord, across web cracks and the dowel action in the longitudinal reinforcement:

$$V = V_c + V_{ai} + V_d \tag{16}$$

The evaluation of the maximum allowable shear force needs iteration since the load applied on the beam is not known in advance. In this paper V in Eq. (15) was equalled V_{max}.

3 Analysis and comparison of models

To assess an agreement of the calculated and experimental results a coefficient $\eta = V_{max}/V_{(1)/(2)}$ was used (where: V_{max} – the maximum shear force from experimental test and $V_{(1)/(2)}$ – the shear capacity calculated according to analysed models). The results corresponding to values $\eta < 1$ indicate the overestimation of the shear strength, while the results $\eta > 1$ confirm the conservative approach of the verified model. Dead loads are not taken into account in the calculated analysis. The analysis was based on the mean strength characteristics of concrete and steel reinforcement . The critical section was assumed in the point of loading. Modulus of elasticity of concrete E_c in model [2] was assumed according to [13]. The comparative analysis of the experimental and analytical results is presented in Table 2 and Figure 5.

Table 2. The experimental and calculated shear strength of tested specimens.

Element	V_{max} [kN]	Model (1)		Model (2)				
		$V_{(1)}$ [kN]	η [-]	$V_{(2)ai}$ [kN]	$V_{(2)c}$ [kN]	$V_{(2)d}$ [kN]	$V_{(2)}$ [kN]	η [-]
G-512-30-15	34.27	40.81	0.84	13.22	4.00	5.51	22.73	1.51
G-316-30-15	31.75	42.49	0.75	13.68	3.82	8.42	25.91	1.22
G-512-30-35	32.47	36.47	0.89	13.46	3.87	5.57	22.90	1.42
G-316-30-35	31.01	36.51	0.85	12.57	3.84	8.36	24.77	1.25
G-316-35-15	31.31	48.35	0.65	15.32	3.67	8.92	27.92	1.12
G-316-35-35	29.90	40.26	0.74	14.10	3.63	8.75	26.48	1.13
G-312/212-30-15	34.78	39.83	0.87	13.15	4.08	5.64	22.87	1.52
S-512-30-15	55.59	76.64	0.73	32.26	12.41	5.57	50.25	1.11
S-316-30-15	52.59	79.88	0.66	32.83	12.06	8.52	53.42	0.98
S-512-30-35	45.24	66.21	0.68	37.74	10.36	5.57	53.67	0.84
S-312/212-30-15	50.93	72.70	0.70	34.98	11.47	5.64	52.09	0.98
S-512-35-15	45.14	83.90	0.54	42.79	9.92	5.79	58.50	0.77
S-316-35-15	44.52	87.47	0.51	41.76	10.05	8.86	60.67	0.73
S-512-35-35	43.40	72.27	0.60	42.17	9.77	5.79	57.74	0.75
S-316-35-35	41.72	75.09	0.56	40.51	9.65	8.86	59.03	0.71
G-318-30-15	38.57	46.93	0.82	12.87	5.20	8.91	26.97	1.43
G-416-30-15	34.77	47.67	0.73	16.39	4.81	7.05	28.25	1.23
G-318-30-35	34.42	40.28	0.85	12.91	4.77	8.85	26.54	1.30
G-318-35-15	33.76	53.43	0.63	16.27	4.43	9.45	30.15	1.12
G-416-35-15	32.43	53.97	0.60	19.33	4.38	7.45	31.17	1.04
S-318-30-15	56.10	90.37	0.62	36.19	14.24	9.16	59.59	0.94
S-318-35-15	47.04	97.62	0.48	46.09	11.78	9.47	67.35	0.70
S-318-35-35	46.89	81.85	0.57	41.13	12.08	9.39	62.60	0.75
G-418-30-15	38.14	53.33	0.72	17.28	5.89	7.24	30.41	1.25
G-318/118-30-15	47.72	51.50	0.93	13.44	7.42	7.33	28.19	1.69
G-418-30-35	39.41	45.25	0.87	14.82	6.28	7.16	28.26	1.39
G-418-35-35	35.14	50.43	0.70	18.16	5.48	7.53	31.17	1.13
S-318/118-30-15	61.79	94.37	0.65	41.75	18.02	7.44	67.21	0.92
S-418-30-35	52.94	86.62	0.61	46.49	15.64	7.44	69.58	0.76

Comparison made according to model [1] (Fig. 5), confirms that all results lie on the danger side (grey area of the chart), both for beams reinforced with GFRP and steel bars. However, shear capacity calculated according to model [2] is underestimated in elements reinforced with GFRP bars, while 92% of RC beams indicated overestimated results. The average ratios of the test results to the calculated values based on the model [1] are: η_m = 0.78 - for GFRP reinforced beams and η_m = 0.61 - for steel RC beams (Table 3). For calculations made according to model [2], the average value of the coefficient η for GFRP reinforced elements is η_m = 1.30, while for steel RC beams η_m = 0.84 (Table 3). In the case of demarking a type of reinforcement, the calculation results in both models have similar dispersion, COV = 13% - 15% (Table 3). In the generalized assessment of calculation models without the division into a type of longitudinal reinforcement, model [2] was more conservative than model [1] (Table 3), but a dispersion of calculated results is significant (COV = 25%). However, the values of shear capacity calculated on the basis of model [1] were significantly overestimated in relation to the experimental results. Most likely, the reason lies in the model assumptions, which were calibrated on a limited number of

concrete classes and do not take into account the effect of aggregate and the bond of reinforcement to various types of concrete.

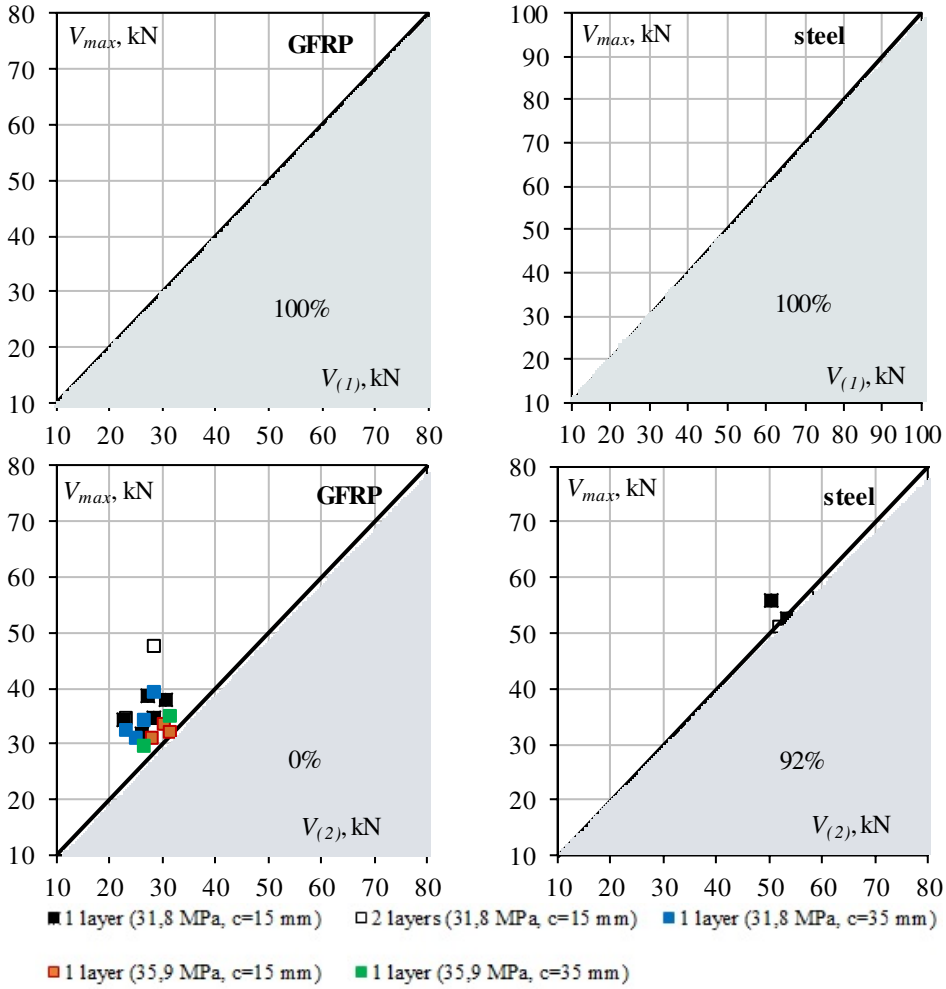

Fig. 5. The experimental and calculated shear capacity according to presented models

Table 3. Statistic assessment of models.

Model	η_{min} [-]	η_{max} [-]	η_m [-]	σ_η [-]	COV [-]
GFRP					
(1)	0.60	0.93	0.78	0.10	0.13
(2)	1.04	1.69	1.30	0.18	0.14
steel					
(1)	0.48	0.73	0.61	0.07	0.12
(2)	0.70	1.11	0.84	0.13	0.15
steel and GFRP (without division)					
(1)	0.48	0.93	0.70	0.12	0.17
(2)	0.70	1.69	1.09	0.27	0.25

Table 2 discloses the individual components of the total shear capacity in model [2]. It can be observed that in the GFRP reinforced beams, the component associated with an aggregate interlock V_{ai} is significantly lower than that in RC beams. The formula (12)

underestimates the aggregate action V_{ai}, which may be due to the fact that it was derived for the steel reinforced members.

Generally, the application of these calculation models to elements reinforced with GFRP bars does not reduce the theoretical values of shear capacity. On the contrary, η factor is usually higher in GFRP reinforced beams than in the corresponding steel reinforced concrete beams (Fig. 6). It is worth noting that for all used reinforcement ratios, similar η values were obtained within one selected model. Therefore, the shear capacity is calculated with similar accuracy. Theoretical models showed slightly lower mean values of the coefficient η in beams with reinforcement ratio $\rho_l \sim 1.4\%$ compared to elements with $\rho_l \sim 1.0\%$ and $\rho_l \sim 1.8\%$ (Fig. 6).

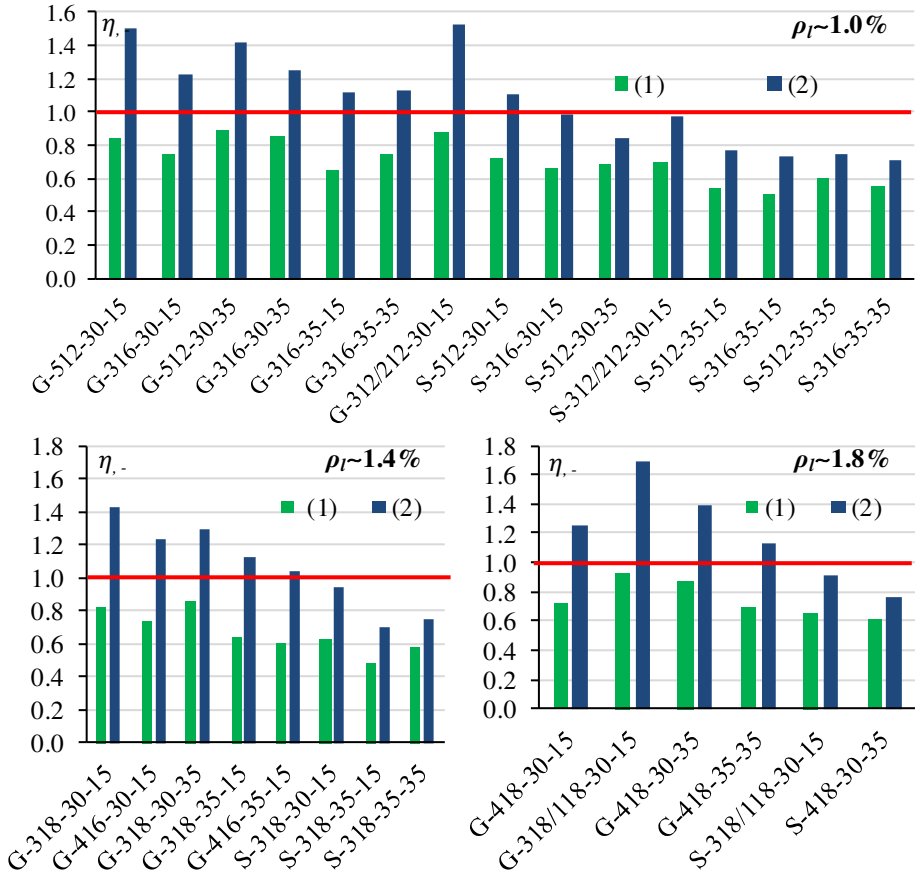

Fig. 6. The comparison of results for models [1] and [2] for longitudinal reinforcement ratio about 1.0, 1.4% and 1.8%

4 Conclusions

Two theoretical models [1], [2] for the shear capacity of beams without stirrups were presented and analyzed. The model [1] was dedicated to the beams without stirrups with variable types of longitudinal reinforcement. However, the comparative analysis performed on the basis the own shear tests of T-section beams without stirrups reinforced with steel and GFRP longitudinal reinforcement showed an overestimation of the model [1] in comparison with experimental results. The model [2] was originally established for steel

RC beams, thus for the GFRP reinforced beams, the shear capacity was underestimated in comparison with experimental values. Both models did not take into account the influence of the flange in T-beams. Therefore, it might be the reason behind the inadequacy of these methods. Although the underestimation of shear capacity for the rectangular beams was expected, it was not confirmed in the comparative analysis. More extensive analysis of this problem was published in the PhD dissertation by M. Kaszubska[14].

References

[1] T. Zhang, D.J. Oehlers, P. Visintin, *Shear Strength of FRP RC Beams and One-Way Slabs without Stirrups*, J. Compos. Constr. **18,** 5 (2014).
[2] Y. Yang, *Shear behaviour of reinforced concrete members without shear reinforcement, a new look at an old problem. PhD thesis*, Delft University of Technology (2014).
[3] ACI 363 *State-of-the-Art Report on High-Strength Concrete (ACI 363R-92)*, ACI J. Proc. **92** (1992).
[4] M. Kaszubska, R. Kotynia, J.A.O. Barros, H. Baghi, *Shear behavior of concrete beams reinforced exclusively with longitudinal glass fiber reinforced polymer bars: Experimental research*, Struct. Concr., **19**, 1, 152–161 (2017).
[5] M. Kaszubska, R. Kotynia, J.A.O. Barros, *Influence of longitudinal GFRP reinforcement ratio on shear capacity of concrete beams without Stirrups*, *Proc. Eng.* **193** (2017).
[6] R. Kotynia, M. Kaszubska, *Research of the flexural reinforcement effect on the shear strength of concrete beams without transverse reinforcement. Report no 23*. Series: Experimental research on concrete elements and structures. Department of Concrete Structures, Lodz University of Technology, Poland Lodz. Publication under patronage of Concrete Structures Section of the Civil Engineering Committee, Polish Academy of Science, 164p (2020).
[7] T. Zhang, *A mechanics based approach for shear strength of RC beams without web reinforcement*, Dep. Rep. **184** (2013).
[8] W. Lucas, D.J. Oehlers, M. Ali, *Formulation of a shear resistance mechanism for inclined cracks in RC beams*, J. Struct. Eng. **137**, 12, (2011).
[9] Z.P. Bažant, H. Ohtsubo, *Stability conditions for propagation of a system of cracks in a brittle solid*, Mech. Res. Commun., **4**, 5, 353–366 (1977).
[10] J. Walraven, *Aggregate Interlock: A theoretical and experimental analysis. PhD Dissertation*, Delft University of Technology (1980).
[11] T. Baumann, H. Rüsch, *Versuche zum Studium der Verdübelungswirkung der Biegezugbewehrung eines Stahlbetonbalkens (Heft 210)* (1970).
[12] E. Mörsch, *Concrete-Steel Construction*. Engineering News Publishing Co. (1909).
[13] EN 1992–1–1, *Eurocode 2: Design of concrete structures. Part 1: General rules and rules for buildings* (2004).
[14] M. Kaszubska, *Analysis of the flexural reinforcement on the shear strength of the concrete beams without transverse reinforcement,* PhD Dissertation, Lodz (2018).